NASA Technical Memorandum 107016

Temperature Dependent Cyclic Deformation Mechanisms in Haynes 188 Superalloy

K. Bhanu Sankara Rao
Lewis Research Center
Cleveland, Ohio

Michael G. Castelli
NYMA, Inc.
Brook Park, Ohio

Gorden P. Allen and John R. Ellis
Lewis Research Center
Cleveland, Ohio

Prepared for the
International Symposium on Inelastic Deformation, Damage, and Life Analysis
cosponsored by the Japanese Society of Mechanical Engineers and
United States Association of Computational Mechanics
Mauna Lani, Hawaii, July 30—August 3, 1995

National Aeronautics and
Space Administration

TEMPERATURE DEPENDENT CYCLIC DEFORMATION MECHANISMS IN HAYNES 188 SUPERALLOY

K. Bhanu Sankara Rao[1]
National Aeronautics and Space Administration
Lewis Research Center
Cleveland, Ohio 44135

Michael G. Castelli
NYMA, Inc.
Engineering Services Division
Brook Park, Ohio 44142

Gorden P. Allen and John R. Ellis
National Aeronautics and Space Administration
Lewis Research Center
Cleveland, Ohio 44135

Abstract

The cyclic deformation behavior of a wrought cobalt-base superalloy, Haynes 188[2], has been investigated over a range of temperatures between 25 and 1000°C under isothermal and in-phase thermomechanical fatigue (TMF) conditions. Constant mechanical strain rates ($\dot{\varepsilon}$) of $10^{-3}s^{-1}$ and $10^{-4}s^{-1}$ were examined with a fully reversed strain range of 0.8%. Particular attention was given to the effects of dynamic strain aging (DSA) on the stress-strain response and low cycle fatigue life. A correlation between cyclic deformation behavior and microstructural substructure was made through detailed transmission electron microscopy. Although DSA was found to occur over a wide temperature range between approximately 300 and 750°C, the microstructural characteristics and the deformation mechanisms responsible for DSA varied considerably and were dependent upon temperature. In general, the operation of DSA processes led to a maximum of the cyclic stress amplitude at 650°C, and was accompanied by pronounced planar slip, relatively high dislocation density, and the generation of stacking faults. DSA was evidenced through a combination of phenomena, including serrated yielding, an inverse dependence of the maximum cyclic hardening with $\dot{\varepsilon}$, and an instantaneous inverse $\dot{\varepsilon}$ sensitivity verified by specialized $\dot{\varepsilon}$-change tests. The TMF cyclic hardening behavior of the alloy appeared to be dictated by the substructural changes occurring at the maximum temperature in the TMF cycle.

Introduction

Application of the cobalt-base superalloy, Haynes 188 in aerospace gas turbine engines necessitates a comprehensive understanding of cyclic deformation under isothermal and thermomechanical loading conditions. Mechanistic based fatigue damage modeling cannot be

[1]National Research Council-NASA Research Associate at Lewis Research Center.

[2]Haynes 188 is a registered trademark of Haynes International, Inc., Kokomo, Indiana.

accurately guided without proper correlation between the cyclic stress response and evolving deformation microstructure. Further, certain combinations of temperature and strain rate could exert a strong influence on the cyclic behavior through the action of individual or simultaneous interaction of various time- and temperature-dependent variables/phenomena such as inelastic deformation, dynamic strain ageing (DSA), creep damage, environmental damage, deformation ratchetting, dynamic precipitation, etc. In order to clarify the effects of some of these processes, isothermal and in-phase thermomechanical fatigue (TMF) tests were conducted in the range 25 to 1000°C at various strain rates on Haynes 188, which culminated in an extensive data base. In this paper, a summary of representative results on the temperature and strain rate dependence of strain controlled isothermal fatigue deformation is given. The corresponding deformation mechanisms at different temperatures are briefly discussed. The temperature dependence of TMF deformation behavior is rationalized on the basis of the cyclic stress response and deformation substructure developed under representative isothermal conditions.

Experimental Details

Wrought Haynes 188 bars of 19 mm dia. with the composition (wt %) 24.43Ni, 21.48Cr, 13.95W, 1.24Fe, 0.01C, 0.75Mn, 0.40Si, 0.012P, 0.002S, 0.034La, 0.002B and balance Co, were solution treated for 1 hr. at 1175°C prior to machining the samples for low cycle fatigue (LCF) testing. The average grain size was ASTM 6. Fully-reversed, total axial strain controlled isothermal LCF tests were performed on 6 mm dia. and 12.5 mm parallel gauge length specimens, at different temperatures in the range 25 to 1000°C, employing a triangular waveform and an axial strain range of 0.80%. The strain rates ($\dot{\varepsilon}$) employed for the isothermal tests included $10^{-4}s^{-1}$ and $10^{-3}s^{-1}$. In-phase TMF tests with a mechanical $\dot{\varepsilon}$ of $10^{-4}s^{-1}$ were conducted on parallel sided tubular specimens featuring an 8.4 and 11.4 mm inner and outer dia., respectively, and a longitudinal gauge length of 12.7 mm. Here, the maximum tensile strain coincided with the maximum temperature, and the maximum compressive strain with the minimum temperature. In the TMF tests, the control of total axial strain was accomplished by continuously providing for compensation of the thermal strain, such that the mechanical strain range was also held constant at 0.80 %. The test specimens were heated with direct induction heating and cooling was accomplished through the use of water cooled grips; no forced air was used.

Samples for TEM examination were obtained from thin slices cut at a distance approximately 1 mm away from the fracture surface. The slices were mechanically thinned down to 250 μm, and then electropolished in a solution containing 10% perchloric acid and 90% methanol, at 22 V and 5°C, in a twin jet apparatus. Thin foils were examined in an electron microscope operating at an acceleration voltage of 120 keV.

Results and Discussion

The cyclic stress response curves collected in Figs. 1 & 2 for two different strain rates illustrate the temperature dependence of the peak tensile stress in successive cycles. The stress amplitudes presented correspond to those values existing at the maximum strain amplitude. At low temperatures ($\leq$ 200°C) for both strain rates, the alloy exhibited a brief period of initial hardening, followed by an extended stage of nearly stable stress response which persisted until the crack nucleation and growth impaired the load-carrying capacity of the specimen, as indicated

by a rapid fall in stress towards the end of the test. In the intermediate temperature domain, which varied depending on $\dot{\varepsilon}$, continuous cyclic hardening occurred until the onset of failure. At very high temperatures, cyclic softening occurred from the first cycle onwards. Softening effects generally commenced at temperatures greater than 900°C and 800°C, at $10^{-3}s^{-1}$ and $10^{-4}s^{-1}$, respectively.

In general, at both the strain rates, the maximum tensile stress decreased with increasing temperature to 300°C, displayed an increase with increasing temperature between 400 and 650°C, and then showed a rapid fall above 750°C. The inelastic strain range developed in the cycle at half-life showed a rapid decrease with a raise in temperature between 300 and 650°C at both strain rates. In tests performed at $\dot{\varepsilon} = 10^{-3}s^{-1}$, the deformation behavior displayed serrations in the plastic portions of stress-strain hysteresis loops between 300 and 850°C, while at the lower $\dot{\varepsilon}$ serrated flow was observed over the much narrower range of 400 to 650°C. The occurrence of DSA was suggested by several observations, including *i*) the maximum cyclic hardening occurred at an intermediate temperature, i.e., 650°C, *ii*) the deformation behavior revealed serrated flow, and *iii*) both the maximum cyclic hardening stress and the inelastic strain range at half-life showed an inverse temperature dependence with strain rate in the intermediate temperature domain. The comparison of maximum stress amplitudes attained at different temperatures in Figs. 1 & 2 revealed an increase in the maximum tensile stress with decreasing $\dot{\varepsilon}$ between 400 and 700°C establishing the negative dependence of maximum stress on $\dot{\varepsilon}$. Above and below this temperature range, the maximum stress decreased with decreasing $\dot{\varepsilon}$. The occurrence of a negative dependence of maximum stress on the $\dot{\varepsilon}$ is a typical manifestation of fatigue deformation accompanying DSA [1-3]. In order to obtain further insight into the macroscopic aspects of DSA during LCF, the "instantaneous" strain rate sensitivity (SRS) of cyclic stress was also examined by conducting instantaneous strain-rate-change tests at several temperatures; these tests were accomplished by only periodically changing the $\dot{\varepsilon}$ to $10^{-4}s^{-1}$ for one cycle and then returning it to the higher $\dot{\varepsilon}$. Thus, a negative SRS would be evidenced by an immediate increase in the cyclic stress amplitude, corresponding to a decrease in $\dot{\varepsilon}$. These tests indicated positive SRS below 300°C, strongly negative between 400 and 650°C, slightly negative at 700 and 750°C and positive again above 800°C. The SRS became substantially negative only in the temperature range where serrated flow occurred at both the strain rates, suggesting the true dependence of DSA on $\dot{\varepsilon}$. Finally, considering all of the phenomenological indicators of DSA discussed above, a DSA domain can be established from approximately 300 to 750°C.

Representative micrographs of the deformation substructure developed below, within, and above the DSA domain at $10^{-4}s^{-1}$ are depicted in Figs. 3 through 6. Below the DSA range, the substructure was made up of distinctly spaced slip bands consisting of dislocation bundles and dipoles (Fig. 3), and a few ill-defined tangles at the intersection of multiple slip bands. The occurrence of bundles and dipoles in slip bands in the absence of cells can be construed as the occurrence of localized cross-slip in the slip bands only. In the DSA domain between 400 and 550°C, dislocations frequently formed planar arrays with well developed stacking faults, Fig. 4. The propensity for planar slip and the formation of stacking faults reached a peak at 550°C. Towards the end of the DSA regime at 600 and 650°C, the dislocation density was very high and the substructures assumed a more homogeneous network, as shown in Fig. 5. DSA has been proposed to occur due to the hinderance of dislocation motion by solute atmospheres [4] or when the dislocations are temporarily held up at local obstacles in the glide plane [5-7]. During DSA, additional dislocations are generated in order to maintain the imposed strain amplitude, leading

to observed increases in dislocation density, such as that shown in Fig. 5. In the DSA regime where planar slip prevailed, the marked cyclic hardening could be attributed to the combined effects of accumulation of dislocations in planar slip bands, uninterrupted initiation of slip bands until the maximum stress is reached, the progressive build up of dislocation pile-ups at grain boundaries with associated internal stresses, and localized strengthening resulting from segregation of solute atoms on stacking faults. At temperatures higher than 850°C, dynamic recovery by thermally activated dislocation climb gained importance leading to the formation of subgrains with sharp walls as depicted in Fig. 6. It must be mentioned that, in the low and intermediate temperature domains up to approximately 700°C, the deformation substructures developed with $\dot{\varepsilon} = 10^{-3}s^{-1}$ clearly displayed similarities to those generated with $\dot{\varepsilon} = 10^{-4}s^{-1}$. In the regime between 750 and 900°C, however, in the high $\dot{\varepsilon}$ tests a greater number of dislocations were found to be anchored by very fine $M_{23}C_6$ precipitates compared to those in low $\dot{\varepsilon}$ tests, where the precipitates showed early signs of growth and over-aging. Dislocation pinning by carbides impeded thermal recovery in the higher $\dot{\varepsilon}$ tests from 750 to approximately 900°C, and led to cyclic hardening, albeit at a declining rate with increasing temperature (Fig. 1). Note, however, that subsequent to initial cyclic hardening, the specimen tested at 900°C with $\dot{\varepsilon} = 10^{-3}s^{-1}$ did experience cyclic softening. Generally speaking, at the higher $\dot{\varepsilon}$, the pronounced substructural features associated with thermal recovery effects could be seen only at temperatures above 900°C.

The evolution of tensile and compressive stresses corresponding to the peak strain amplitudes in the in-phase TMF tests conducted over different temperature intervals, ΔT, (350-550, 400-650, 500-750 and 600-850°C) are summarized in Fig. 7; tensile stress response curves of selected isothermal tests are also included to facilitate comparisons. In the TMF test with ΔT = 350-550°C, the minimum and maximum temperatures were below and within the DSA range, respectively, while in the 500-750 and 600-850°C tests the lower and higher peak temperatures were within and above the DSA range, respectively (for $\dot{\varepsilon} = 10^{-4}s^{-1}$). The test with ΔT = 400-650°C is entirely within the DSA range. In all the isothermal tests, the tensile and compressive stress amplitudes in the same cycle were nominally equivalent. In contrast, in the in-phase TMF tests the compressive stress amplitudes (experienced at the lower temperatures) were higher than the tensile stress amplitudes and thus led to compressive mean stresses. The mean stress was mild in the 350-550°C test, whereas the other TMF tests experienced significant mean stresses which tended to increase with cycling. The mean stresses became particularly large when the maximum temperature of the TMF cycle was above, and minimum temperature was within, the DSA range. In all the TMF tests, the maximum strain tensile stresses experienced at the maximum temperature of the cycles were nearly identical to those attained in corresponding isothermal tests; however, the number of cycles needed to attain this stress level in each of the TMF tests was less than those in the isothermal tests. In contrast, the maximum compressive stresses attained in the TMF tests were not well represented by the isothermal tests performed at the corresponding temperatures. That is, the low-temperature peak stresses experienced greater increases in the TMF tests showing significant deviations from the corresponding isothermal tests. The maximum hardening rates and magnitudes experienced by the TMF compressive peaks at 400°C substantially exceeded those displayed isothermally at 400°C (745 versus 457 MPa, respectively). This is a significant result considering that the 400-650°C cycle is entirely within the DSA range. This "unbounded" behavior is clear evidence of thermomechanical path dependence, as the material behavior at 400°C is profoundly influenced by the deformation substructure developed under TMF conditions in the DSA range. Although the compressive peak stresses in the 500-750°C cycle showed a considerable increase due to the DSA effects as

compared to the isothermal test at 500°C, the amount of hardening was far less than that obtained in the 400-650°C TMF test, because part of the cycle lied in the range where dynamic recovery effects became operative. In the TMF test with ΔT = 600-850°C, where the main fraction of the cycle involves loading above the DSA range, the recovery effects seem to have become substantial, thus causing the hardening mechanisms associated with DSA to be less effective at the lower end of the cycle. In fact, the large mean stresses in the two higher ΔT ranges develop as a consequence of conditions promoting hardening due to DSA at one end of the cycle and softening due to recovery at the other end.

Concluding Remarks

Isothermal LCF and in-phase TMF experiments under fully reversed 0.8% mechanical axial-strain control with strain rates ($\dot{\varepsilon}$) of $10^{-3}s^{-1}$ and $10^{-4}s^{-1}$ were conducted on Haynes 188 over the temperature range 25-1000°C. The fatigue deformation and stress response clearly indicated the operation of DSA processes, nominally between the temperatures of 300 and 750°C and was evidenced through a combination of phenomena, including serrated yielding, an inverse dependence of maximum cyclic hardening with $\dot{\varepsilon}$, and an inverse instantaneous $\dot{\varepsilon}$ sensitivity. A maximum LCF cyclic stress amplitude was experienced at 650°C for both strain rates. The occurrence of DSA was found to be associated with pronounced planar slip, generation of stacking faults, and relatively high dislocation densities. The in-phase TMF behavior of the alloy seems to have been dictated by the substructural changes occurring at the maximum temperature in the TMF cycle.

References

[1] M.G. Castelli, R.V. Miner and D.N. Robinson, ASTM STP 1186, 1993, p.106.
[2] R. Zauter, F. Petry, H.-J. Christ and H. Mughrabi, Ibid, p.70.
[3] K. Bhanu Sankara Rao, M. Valsan, R. Sandhya, S.L. Mannan and P. Rodriguez, High Temperature Materials and Processes, Vol.7, 1986, p.171.
[4] A.H. Cottrell: Philos. Mag., 1953, Vol.44, pp 829-835.
[5] A. van den Beukel: Acta. Metall., 1980, Vol.28, pp. 965-969.
[6] A. van den Beukel and U.F. Kocks: Acta Metall., 1982, Vol.30, pp. 1027-1034.
[7] U.F. Kocks, A.S. Argon and M.F. Ashby: Prog. Mater. Sci., 1975, Vol.19, pp 1-49.

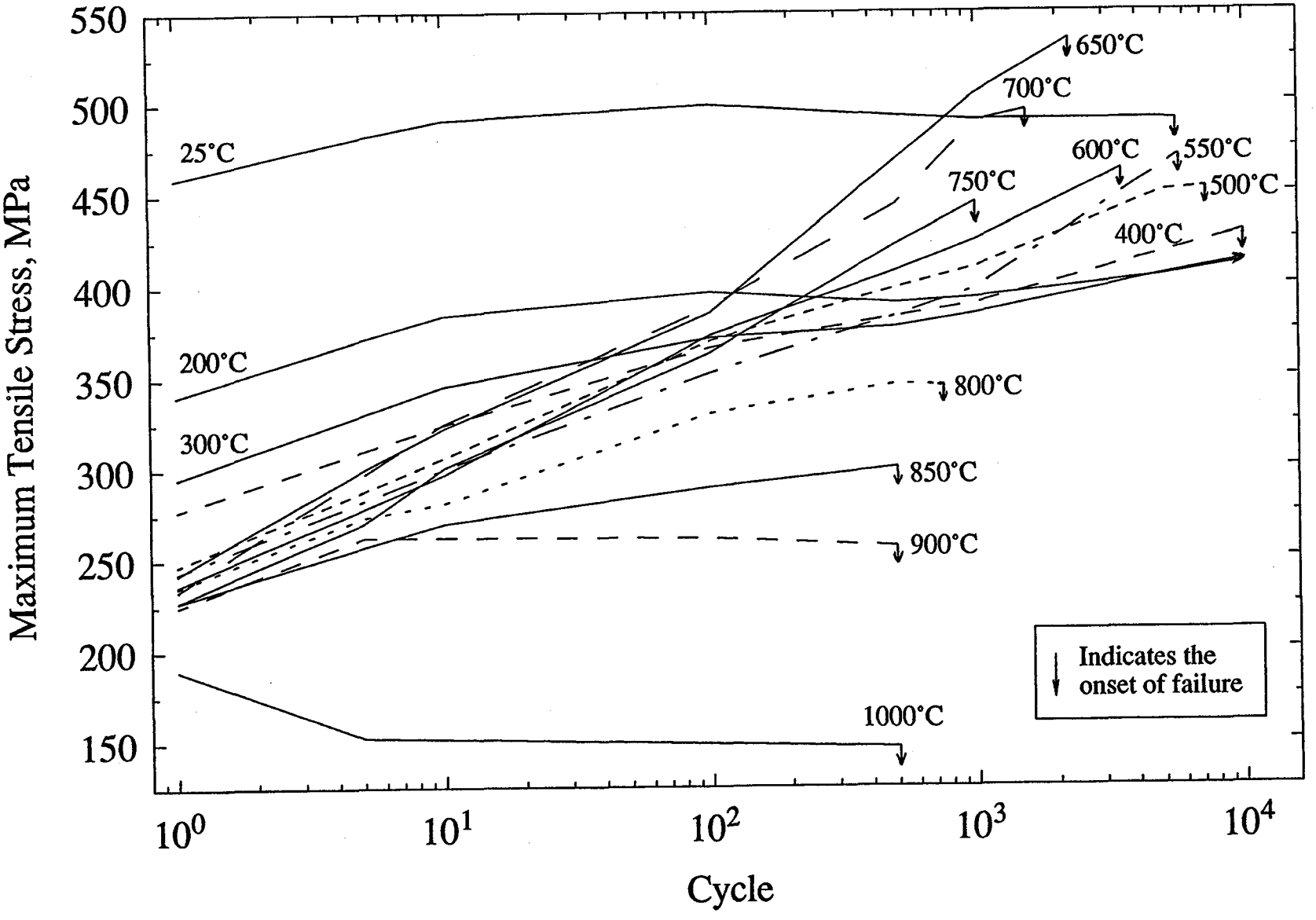

Fig. 1.--Cyclic maximum tensile stress during isothermal LCF with $\Delta\epsilon$=0.8% and $\epsilon=10^{-3}s^{-1}$.

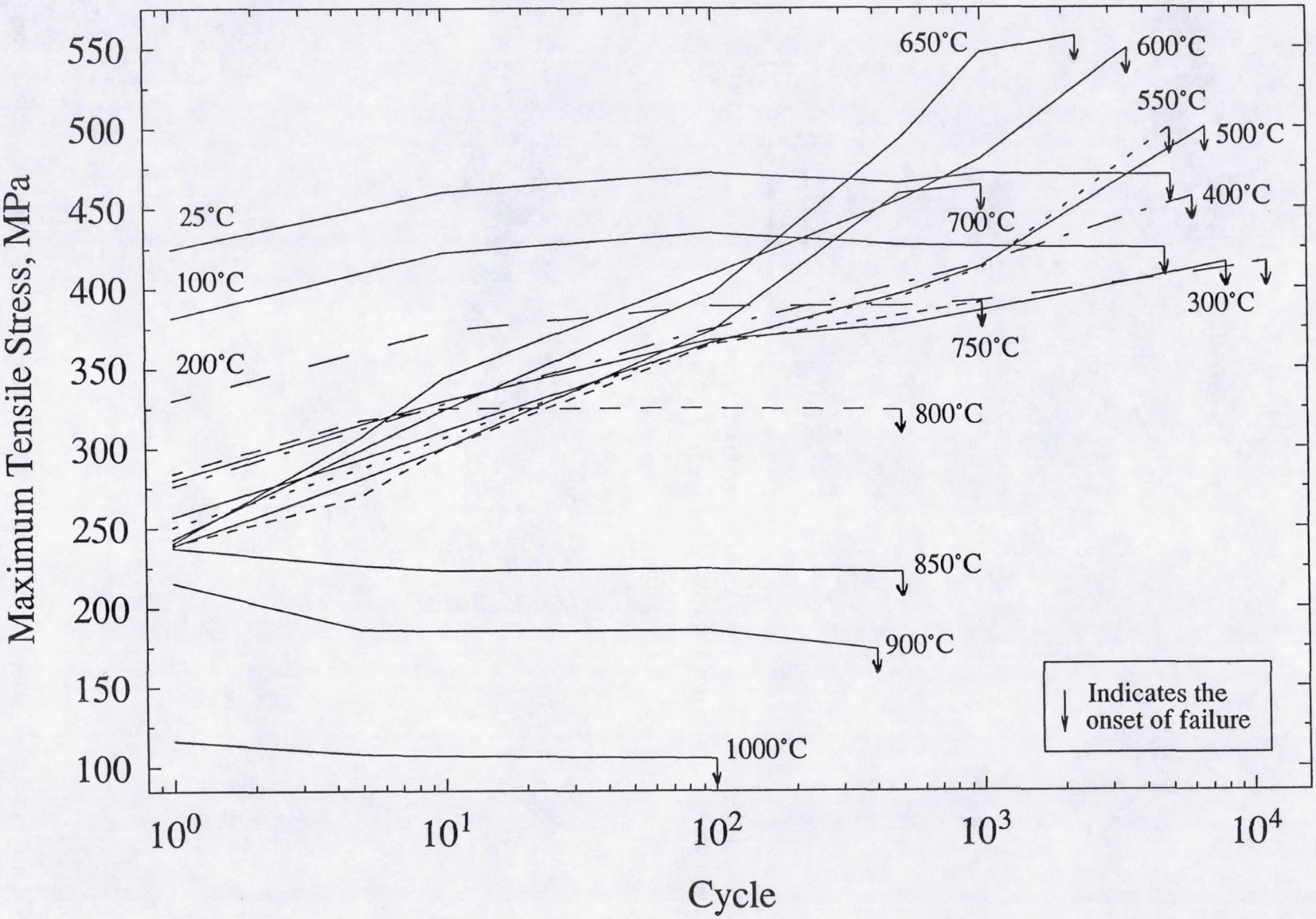

Fig. 2.--Cyclic maximum tensile stress during isothermal LCF with $\Delta\epsilon$=0.8% and $\epsilon=10^{-4}s^{-1}$.

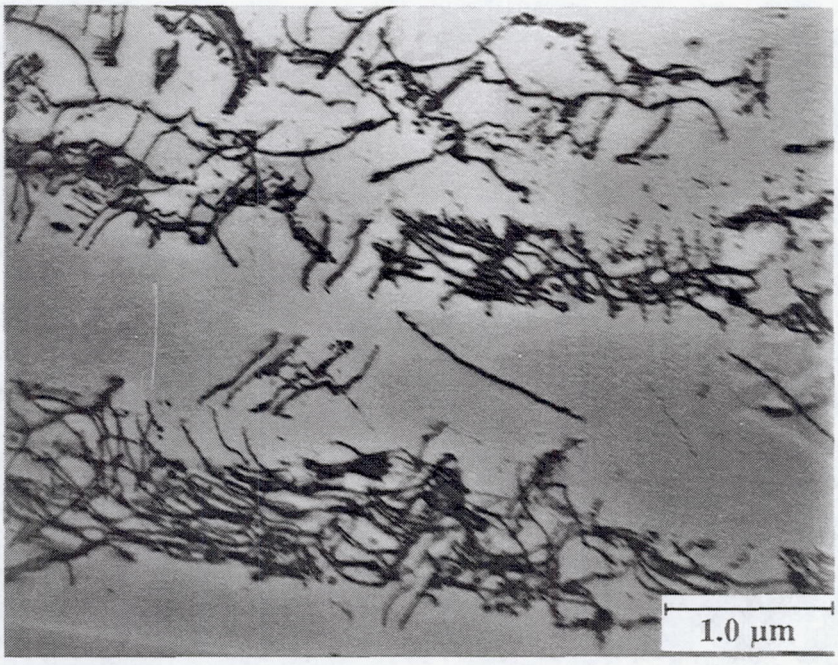

Fig. 3.--TEM Micrograph taken from an LCF specimen tested at 25°C showing dislocation dipoles and bundles in planar slip bands.

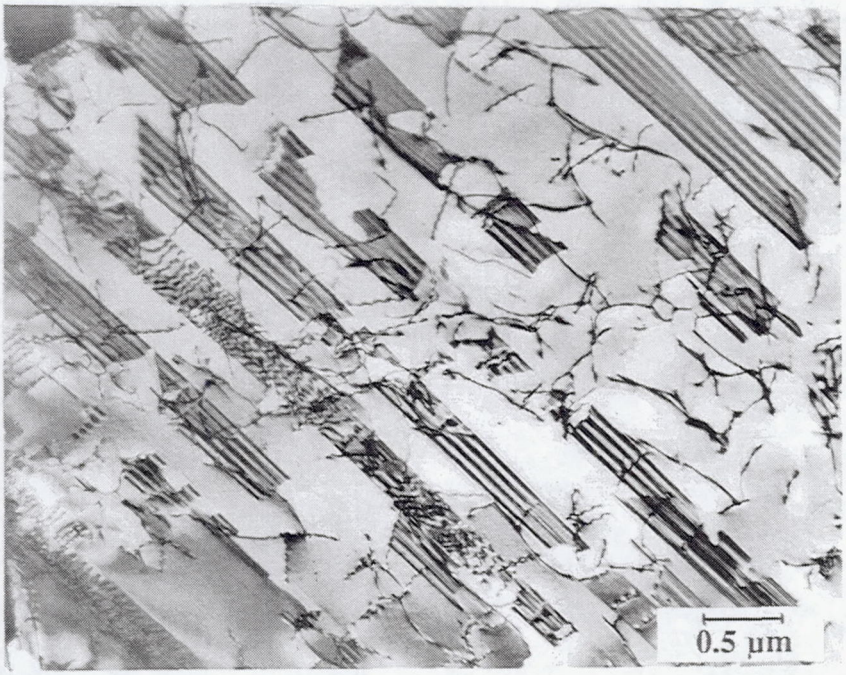

Fig. 4.--TEM Micrograph taken from an LCF specimen tested at 400°C showing planar arrays of dislocations in slip bands and stacking faults.

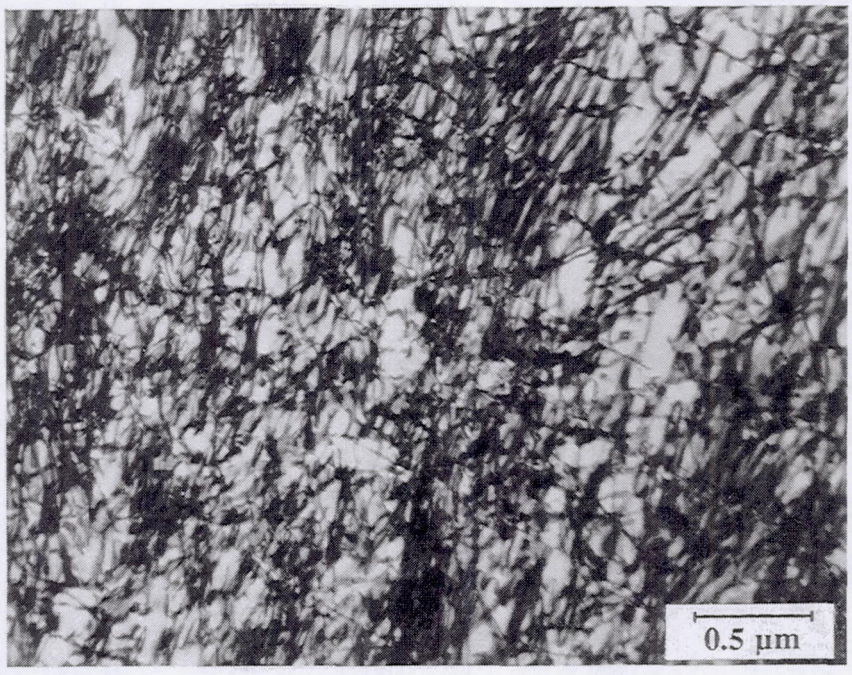

Fig. 5.--TEM Micrograph taken from an LCF specimen tested at 650°C showing a very high density homogeneous network of dislocations.

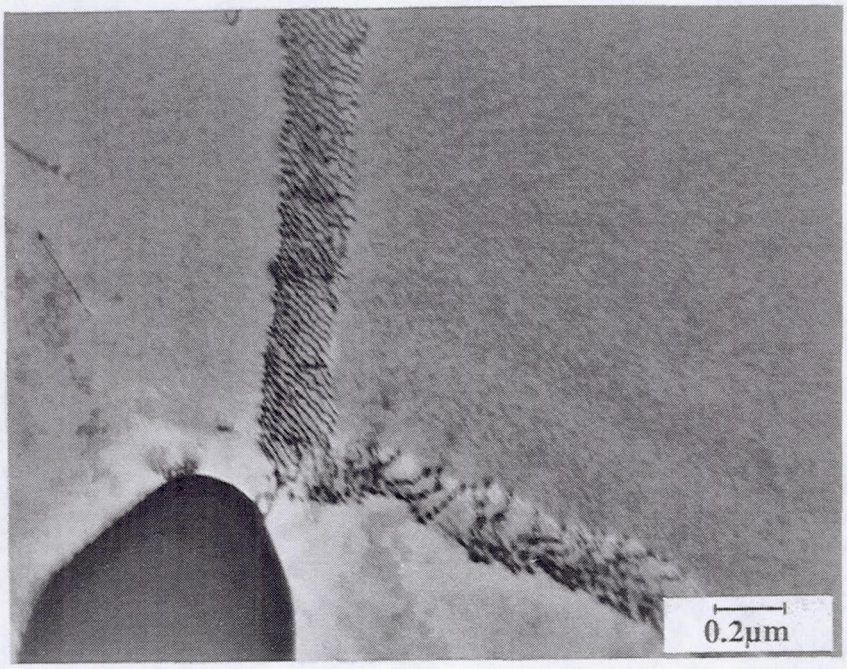

Fig. 6.--TEM Micrograph taken from an LCF specimen tested at 1000°C showing subgrain walls with orderly dislocation arrangements.

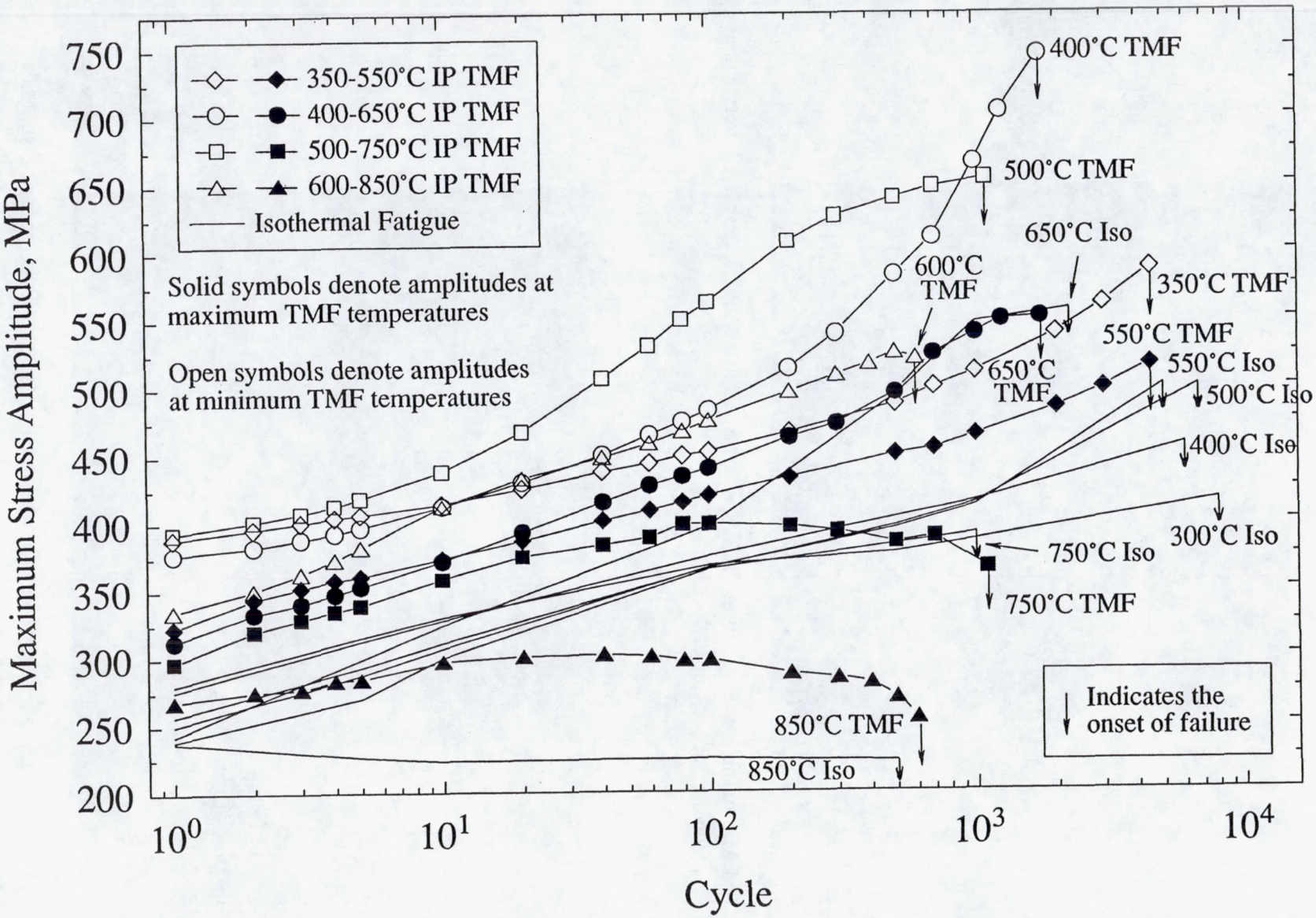

Fig. 7.--Cyclic maximum stress amplitudes of TMF and LCF with $\Delta\epsilon$=0.8% and $\dot{\epsilon}=10^{-4}s^{-1}$.

REPORT DOCUMENTATION PAGE

Form Approved
OMB No. 0704-0188

1. AGENCY USE ONLY (*Leave blank*)	2. REPORT DATE	3. REPORT TYPE AND DATES COVERED
	August 1995	Technical Memorandum

4. TITLE AND SUBTITLE

Temperature Dependent Cyclic Deformation Mechanisms in Haynes 188 Superalloy

5. FUNDING NUMBERS

WU–505–63–5B

6. AUTHOR(S)

K. Bhanu Sankara Rao, Michael G. Castelli, Gorden P. Allen, and John R. Ellis

7. PERFORMING ORGANIZATION NAME(S) AND ADDRESS(ES)

National Aeronautics and Space Administration
Lewis Research Center
Cleveland, Ohio 44135–3191

8. PERFORMING ORGANIZATION REPORT NUMBER

E–9802

9. SPONSORING/MONITORING AGENCY NAME(S) AND ADDRESS(ES)

National Aeronautics and Space Administration
Washington, D.C. 20546–0001

10. SPONSORING/MONITORING AGENCY REPORT NUMBER

NASA TM–107016

11. SUPPLEMENTARY NOTES

Prepared for the International Symposium on Inelastic Deformation, Damage, and Life Analysis cosponsored by the Japanese Society of Mechanical Engineers and United Stated Association of Computational Mechanics, Mauna Lani, Hawaii, July 30—August 3, 1995. K. Bhanu Sankara Rao, NASA Lewis Research Center and National Research Council—NASA Research Associate at Lewis Research Center; Michael G. Castelli, NYMA, Inc., 2001 Aerospace Parkway, Brook Park, Ohio 44142 (work funded by NASA Contract NAS3–27186); Gorden P. Allen and John R. Ellis, NASA Lewis Research Center. Responsible person, John R. Ellis, organization code 5220, (216) 433–3340.

12a. DISTRIBUTION/AVAILABILITY STATEMENT

Unclassified - Unlimited
Subject Category 39

This publication is available from the NASA Center for Aerospace Information, (301) 621–0390.

12b. DISTRIBUTION CODE

13. ABSTRACT (*Maximum 200 words*)

The cyclic deformation behavior of a wrought cobalt-base superalloy, Haynes 188, has been investigated over a range of temperatures between 25 and 1000°C under isothermal and in-phase thermomechanical fatigue (TMF) conditions. Constant mechanical strain rates ($\dot{\varepsilon}$) of $10^{-3}s^{-1}$ and $10^{-4}s^{-1}$ were examined with a fully reversed strain range of 0.8%. Particular attention was given to the effects of dynamic strain aging (DSA) on the stress-strain response and low cycle fatigue life. A correlation between cyclic deformation behavior and microstructural substructure was made through detailed transmission electron microscopy. Although DSA was found to occur over a wide temperature range between approximately 300 and 750°C, the microstructural characteristics and the deformation mechanisms responsible for DSA varied considerably and were dependent upon temperature. In general, the operation of DSA processes led to a maximum of the cyclic stress amplitude at 650°C, and was accompanied by pronounced planar slip, relatively high dislocation density, and the generation of stacking faults. DSA was evidenced through a combination of phenomena, including serrated yielding, an inverse dependence of the maximum cyclic hardening with $\dot{\varepsilon}$, and an instantaneous inverse $\dot{\varepsilon}$ sensitivity verified by specialized $\dot{\varepsilon}$-change tests. The TMF cyclic hardening behavior of the alloy appeared to be dictated by the substructural changes occuring at the maximum temperature in the TMF cycle.

14. SUBJECT TERMS

Dynamic strain aging; Fatigue; Deformation substructures; Haynes 188

15. NUMBER OF PAGES

12

16. PRICE CODE

A03

17. SECURITY CLASSIFICATION OF REPORT	18. SECURITY CLASSIFICATION OF THIS PAGE	19. SECURITY CLASSIFICATION OF ABSTRACT	20. LIMITATION OF ABSTRACT
Unclassified	Unclassified	Unclassified	